Ultrasensitive Synthetic Protein Regulatory Networks Using Mixed Decoys

Michelle S. Lu,[†,‡] Jonathon F. Mauser,[†,§] and Kenneth E. Prehoda[†,§,*]

[†]Institute of Molecular Biology, [‡]Department of Biology, and [§]Department of Chemistry, University of Oregon, Eugene, Oregon 97403, United States

S *Supporting Information*

ABSTRACT: Cellular protein interaction networks exhibit sigmoidal input−output relationships with thresholds and steep responses (i.e., ultrasensitivity). Although cooperativity can be a source of ultrasensitivity, we examined whether the presence of "decoy" binding sites that are not coupled to activation could also lead to this effect. To systematically vary key parameters of the system, we designed a synthetic regulatory system consisting of an autoinhibited PDZ domain coupled to an activating SH3 domain binding site. In the absence of a decoy binding site, this system is non-ultrasensitive, as predicted by modeling of this system. Addition of a high-affinity decoy site adds a threshold, but the response is not ultrasensitive. We found that sigmoidal activation profiles can be generated utilizing multiple decoys with mixtures of high and low affinities, where high affinity decoys act to set the threshold and low affinity decoys ensure a sigmoidal response. Placing the synthetic decoy system in a mitotic spindle orientation cell culture system thresholds this physiological activity. Thus, simple combinations of non-activating binding sites can lead to complex regulatory responses in protein interaction networks.

KEYWORDS: *ultrasensitivity, decoy, threshold, spindle orientation*
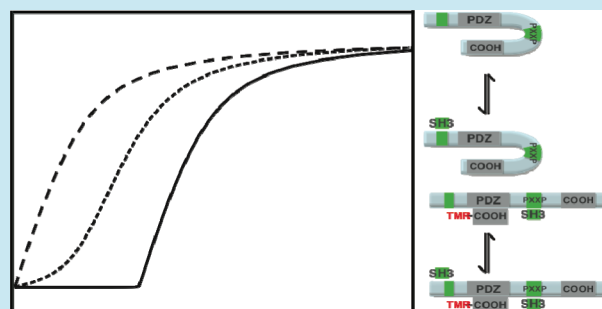
Ultrasensitivity is a common property of cellular signaling systems, yet its molecular origins are poorly understood. Koshland and Goldbeter proposed the term "ultrasensitivity" to describe any system that exhibits a sigmoidal input−output relationship[1−3] (Figure 1A). Sigmoidal activation profiles contain thresholds and steep activation profiles, both of which are thought to be important for biological regulatory systems.[4] Thresholds serve to buffer input noise and offset the response to higher concentration regimes, while sharp responses lead to large output changes over a narrow range of input. These two qualities are necessary for many biological phenomena that exhibit all-or-none behavior, including *Xenopus* oocyte maturation,[5,6] cell-cycle regulation,[7] and binding of oxygen to hemoglobin.[8] While ultrasensitive responses are crucial for the regulation of cell signaling, the molecular mechanisms responsible for translating input gradients into sharp responses are still being uncovered.

Ultrasensitive responses are generally thought to be a product of complex regulatory mechanisms such as feedback loops or cooperativity.[1,9] While cooperative, multistep, and zero-order mechanisms are common sources of ultrasensitivity,[2] simpler mechanisms can also generate sigmoidal response profiles. For example, the sequestration of transcriptional activators is sufficient to generate the ultrasensitive response of a synthetic genetic network,[10] whose ultrasensitivity is measured by the commonly used Hill coefficient.[11] Competition effects are not limited to genetic networks and can provide a means of ultrasensitive regulation of enzyme activity. Competition for substrate phosphorylation sites by the kinase Cdk1 has been reported as the source for the ultrasensitive inactivation of Wee1.[12]

While it has been shown that basic mechanisms such as protein sequestration and substrate competition can generate ultrasensitive profiles, they have been demonstrated in systems controlled either transcriptionally or by post-translational modifications. Transcription and post-translational modifications are common means of cellular regulation, but many cellular decisions rely on rapid simple binary protein interactions.[13−16] Binary protein interactions produce graded binding behaviors (hyperbolic, Michaelis−Menten-type) because they are the product of individual binding interfaces.[17] However, combinations of simple protein interactions can produce complex, nonlinear behaviors such as ultrasensitivity through a simple competition mechanism, much like that seen in the ultrasensitive inactivation of Wee1.

The MAPK and Wee1 signaling cascades utilize "decoy" phosphorylation sites to generate ultrasensitivity. Decoy phosphorylation sites are recognized by the upstream kinase but are not coupled to functional output, instead functioning to buffer the input signal to generate an ultrasensitive response. Much like decoy phosphorylation sites, protein interaction
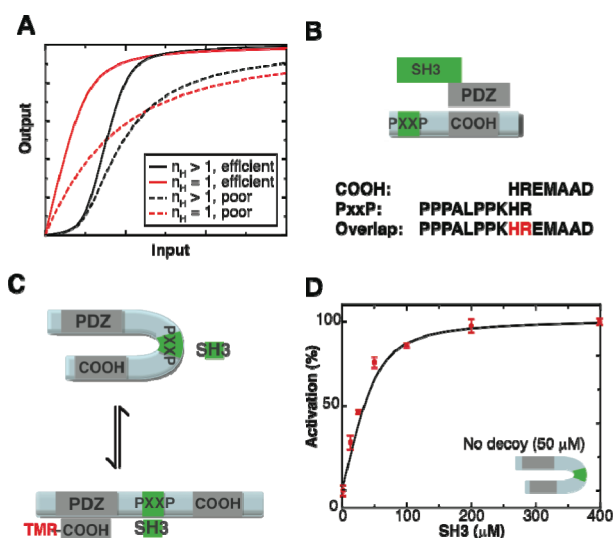
Figure 1. Defining ultrasensitivity and the design and construction of the synthetic regulatory systems. (A) Ultrasensitive profiles (black) are sigmoidal in shape, exhibiting a threshold, and are generally characterized by a Hill coefficient greater than 1, unlike hyperbolic profiles (red). Both hyperbolic and ultrasensitive curves can behave as efficient switches (solid lines) or poor switches (dashed). (B) Overlapping sequences allow for mutually exclusive binding of the SH3 domain or the *cis* PDZ domain to the C-terminal region of the synthetic regulatory system. (C) Simplified graphical representation of the end states in the activation process. The PDZ domain forms an intramolecular interaction with a *cis* PDZ ligand (COOH) to produce an autoinhibited state. SH3 binding to the polyproline motif (PxxP) occludes the intramolecular interaction, exposing the PDZ domain and allowing it to bind a *trans* PDZ ligand. Fluorescent dye-labeled *trans* PDZ ligand (TMR-COOH) binding can be followed by anisotropy to measure the "activated" state (activated but SH3-unbound state is omitted for clarity but was included in the analytical modeling in the Supporting Information). (D) The synthetic regulatory system exhibits a non-ultrasensitive activation profile with a K_{act} of 31 μM (error bars represent SEM from three independent measurements). The synthetic regulatory system is present at 50 μM; 400 μM SH3 corresponds to eight times the repressed polyproline site. The solid line represents the predicted behavior of the system based on the analytical model (see methods and Supporting Information) for the system shown in the schematic using the parameters shown in Table 1. It is not the best fit to the data. All affinities used in the modeling correspond to experimentally measured affinities listed in Table 1.

domains can also serve as sequestering agents to buffer the input signal to generate complex, nonlinear responses. While mathematical modeling supports protein–protein interaction decoy-based ultrasensitivity,[17] the only example of a natural protein–protein interaction pathway to utilize the decoy mechanism to generate ultrasensitivity is the mitotic spindle orientation protein Partner of Inscuteable (Pins).[18] Pins contains three GoLoco motifs, one of which is coupled to activation by the heterotrimeric G-protein α subunit Gαi, while the remaining two GoLoco motifs serve as decoy binding sites for the activating Gαi molecule. The decoy sites bind and sequester Gαi from the activation site, thresholding Pins activation to generate an ultrasensitive profile that can be fit to the Hill equation. The relative affinities and the quantity of decoy domains in a system determine the degree of thresholding, and in the case of Pins, the affinities of the GoLoco domains for Gαi have been appropriately "tuned" to

generate an ultrasensitive response. Thus, simple binary protein interactions can be a source of ultrasensitivity.

While Pins has supplied valuable insight into the decoy mechanism, it remains the only example, natural or otherwise, of a protein-interaction-based competition mechanism capable of generating ultrasensitivity. Is it possible to construct a synthetic system to thoroughly study the decoy mechanism? The construction of synthetic systems that exhibit complex input/output behaviors using protein modularity has been previously reported, where multiple modular domains of an engineered protein were reported to act cooperatively to generate ultrasensitive input/output control.[19] Here we generate an artificial regulatory system using simple protein interaction domains and overlapping binding sites to systematically examine how decoy domains contribute to the input threshold and ultrasensitivity of a system.

We use a synthetic regulatory pathway, along with a modeling approach, to examine whether ultrasensitivity can be generated in synthetic protein interaction networks without cooperativity. We find that the relative affinity of the decoy domains determines the overall shape of the activation profile. Although the synthetic decoy-based systems can be ultra-sensitive with large apparent Hill coefficients, we find that the threshold is the most readily manipulated in this type of regulatory system. In contrast, the steepness of the input/output relationship is limited to a relatively narrow range in this type of pathway. By independently altering these two characteristics, thresholds and steepness, we evaluate their relative contribution to the Hill coefficient, which is the most commonly used measure of ultrasensitivity. Finally, we examine the effects of decoys in our synthetic regulatory pathways in a physiological context using a cell culture assay. We find that decoys can threshold biological activities, such as the spindle orientation activity of Pins in S2 cells. Together, the *in vitro* studies, analytical modeling, and *in vivo* work demonstrate that simple binary protein interactions can tune several parameters of a response.

■ RESULTS AND DISCUSSION

We used an approach combining synthetic biology and analytical modeling to comprehensively explore decoy-based ultrasensitivity. A synthetic system can be precisely controlled to minimize the number of variables being tested,[19] whereas modeling can highlight parameters important for the phenomenon being examined.[10,20] To thoroughly examine decoy-based ultrasensitivity, we built a synthetic regulatory pathway composed of readily available modular domains whose properties (binding partners, affinities, etc) have been extensively characterized. The design of the synthetic regulatory pathway is modular in nature, which allowed for its easy manipulation so that we could systematically test the effects of decoys on ultrasensitivity.

In order to characterize the synthetic regulatory pathway, we developed an *in vitro* biochemical assay as well as an *in vivo* cell biological assay to test the effects of various decoys on thresholding and ultrasensitivity. The *in vitro* assay is based on fluorescence anisotropy using bacterially purified proteins and served as a quantitative method for examining decoy-based ultrasensitivity, whereas the *in vivo* studies highlight the functional consequence of decoy-based ultrasensitivity in a more physiological context. In addition to the biochemistry and cell biology, we analytically modeled the synthetic regulatory pathways, incrementally varying several parameters to fully

66

dx.doi.org/10.1021/sb200010w | *ACS Synth. Biol.* 2012, 1, 65−72

Table 1. Characteristics of the Modular Domains and Their Ligands Used for the Construction of the Synthetic Regulatory Pathways

domain	origin and sequence	ligand(s)	K_d (μM)	ref
PDZ	Par-6 residues 156−255	TMR-CGYPKHREMAVDSP	6	24
		TMR-CGYPKHREMAAD	15	measured[a]
		PPPALPPKHR	1.57	25, 26
SH3	Crk residues 134−191	PPALPPKK	2.1	25, 26
		PPPALPPKRRR	0.1	25, 26
		PPPVPPRR	10	26, 27
PDZ-PxxP-COOH	[Par-6 156−255]-PPPALPPKHREMAAD	TMR-CGYPKHREMAVDSP	48	measured[a]

[a]Affinities measured in *trans* (see Methods).

understand the effects of decoy domains. We found that combining analytical modeling, biochemistry, and cell biology provided a comprehensive analysis of the decoy mechanism and how decoys can be tuned to generate ultrasensitivity.

To construct a system that can be manipulated *in vitro* to test the role of decoy sites in ultrasensitive activation, we designed an "autoinhibited" protein based on a PDZ protein interaction domain. We utilized autoinhibition because it is a common mechanism in signaling pathways in which intramolecular interactions regulate activity.[21] We also utilized PDZ domains because they and their binding partners, short C-terminal sequences,[22] have been well characterized and are readily available. We engineered autoinhibition into the synthetic system using a sequence overlap strategy,[23] where we constructed a fusion protein containing the *Drosophila* Par-6 PDZ domain and a modified PDZ ligand sequence HREMAAD from *Drosophila* Stardust (Sdt).[24] Between the PDZ domain and its ligand sequence, we included an overlapping proline-rich sequence PPPALPPKHR that binds the mouse Crk SH3 domain, with a dissociation constant of 1.57 μM,[25,26] with the goal of disrupting the intramolecular interaction when the SH3 domain binds its target (Figure 1B). The overlapping PDZ ligand and proline-rich sequence permits the mutually exclusive binding of either the *cis* PDZ domain or *trans* SH3 domain at this site, forming a favorable intramolecular interaction that would occlude the SH3 binding site (Figure 1C). The PDZ domain has an approximately 3-fold lower affinity for its *cis* ligand than the fluorescently labeled *trans* ligand, when measured in *trans* (Table 1), so that the system can be more readily activated (effective concentration effects favor the intramolecular interaction).

We used the mouse Crk SH3 domain as the activator and measured output activity using the fluorescence anisotropy of a tetramethyl rhodamine (TMR)-labeled PDZ ligand peptide. Consistent with the presence of autoinhibition in this system, the repressed PDZ domain's affinity for its *trans* ligand is approximately 8-fold lower than the free PDZ domain because of competition with the intramolecular ligand (table 1). The SH3 domain activates the system, and the affinity of the fluorescent peptide for the PDZ domain increases upon SH3 domain binding, resulting in a graded, non-ultrasensitive activation profile (Figure 1D). We also analytically modeled this synthetic regulatory pathway (as well as the others discussed below) using the affinities shown in Table 1 and found the modeling to be in excellent agreement with the experimental findings (Figure 1D, solid line). We next examined whether simple competition could introduce elements of ultrasensitive behavior into our system by adding various SH3 ligands.

To determine the effect of decoy sites on the activation of our synthetic regulatory system, we introduced SH3 binding sites N-terminal to the PDZ domain in regions where SH3 interaction does not influence PDZ activation (Figure 2A). We
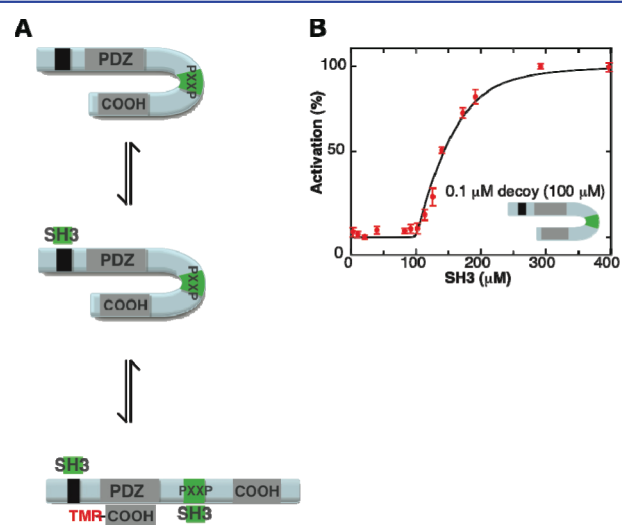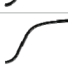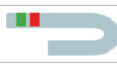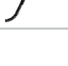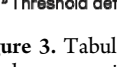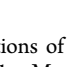

Figure 2. High-affinity decoy sites threshold activity. (A) Graphical representation of end states in the activation sequence. The high-affinity decoy (black) becomes fully saturated with the activating SH3 domain before activation. (B) A high-affinity decoy ($K_d^{SH3} = 0.1$ μM, black) thresholds the activation profile by the concentration of decoy in the reaction (error bars represent SEM from three independent measurements). The total concentration of the system is 100 μM, which corresponds to a total of 100 μM decoy domains ($K_d^{SH3} = 0.1$ μM) and 100 μM repressed polyproline motifs. The solid line represents the predicted behavior of the system based on the analytical model (see Methods and Supporting Information) for the system shown in the schematic using the parameters shown in Table 1. It is not the best fit to the data. All affinities used in the modeling correspond to experimentally measured affinities listed in Table 1.

initially examined the effect of adding a single decoy site with the sequence PPPALPPKRRR at an intrinsic affinity ($K_d^{SH3} = 0.1$ μM) higher than that of the activating SH3 binding site (when measured in isolation, $K_d^{SH3} = 1.57$ μM) and found that this introduces a threshold to the graded response (Figure 2B). The threshold corresponds to the concentration of the synthetic regulatory pathway (and therefore the decoy), indicating that the SH3 activator binds the decoy until it is saturated before binding the activation site. An inflection point in the response profile of this system is predicted by modeling (Supporting Information) and arises because the decoy acts as a strong stoichiometric sink (Figure 2B, solid line). Addition of another high-affinity decoy site causes the threshold to be

Pathway	Decoys No.	K_d (µM)	K_{act} (µM)	n_H	Steepness[a] (10^{-1} % activity/SH3)	Threshold[b] [SH3] (µM)	Profile
(50 µM)	----	----	31	1	12.5	1	hyperbolic
(50 µM)	1	0.1	70	1	12.4	44	offset hyperbolic
(100 µM)	1	0.1	140	1	9	107	offset hyperbolic
(50 µM)	1	2.1	73	2.5	9.5	22	sigmoid
(50 µM)	1	10	51	1	0.4	2.5	hyperbolic
(50 µM)	2	0.1	190	1	8.3	104	offset hyperbolic
(50 µM)	2	2.1	176	3.9	5.5	55	sigmoid
(50 µM)	1, 1	2.1, 0.1	140	3.9	6.7	71	sigmoid
(50 µM)	1, 1	2.1, 10	71	2	5.3	18	sigmoid
(75 µM)	1, 2	2.1, 0.1	250	4.5	7.8	177	sigmoid
(50 µM)	3	2.1	122	2.8	5.3	35	sigmoid
(50 µM)	1, 2	10, 2.1	121	2.6	5.3	25	sigmoid
(50 µM)	1, 2	0.1, 2.1	202	3.7	4.8	93	sigmoid

[a] Steepness defined as slope at K_{act}
[b] Threshold defined as 10% maximal activation

Figure 3. Tabular illustration summarizing the characteristics of synthetic regulatory pathways containing various combinations of decoy domains. We have ommited the PDZ, COOH, and PXXP domains from the regulatory pathway depictions for clarity. The 0.1 µM affinity decoy is represented as a black square, the 2.1 µM affinity decoy as a green square, and the 10 µM affinity decoy as a red square.

further shifted to higher activator concentration but does not alter the overall shape of the activation profile (Figure 3).

These results demonstrate that decoy sites can introduce thresholds, which is a hallmark feature of ultrasensitive responses. However, the profiles of the synthetic pathways containing the nanomolar high-affinity (0.1 µM) decoy are not sigmoidal and therefore do not meet Koshland and Goldbeter's original definition of "ultrasensitive," which is still widely used today. Instead, the profile resembles an offset, graded curve that is poorly fit by the Hill equation, which serves as a common analysis method for ultrasensitivity (the use of the Hill analysis to measure ultrasensitivity is discussed below). Thus, high affinity decoys generate thresholds by shifting the start of the graded response to higher activator concentration but do not generate ultrasensitivity.

In order to generate truly sigmoidal responses, we reasoned that lower affinity (micromolar range) decoys might "blur" the transition between the threshold and activation region by allowing activation before the decoys had become fully saturated (Figure 4A,B). We tested this idea by adding lower affinity (2.1 µM) decoys to the synthetic regulatory system. By lowering the affinity of the decoy site to 2.1 µM from 0.1 µM such that it approximates the affinity of the activation site (K_d^{SH3} = 1.57 µM), it is possible to obtain intermediate activation states where there is a mixture of decoy-bound repressed, decoy-bound activated, and decoy-unbound activated states, generating canonical ultrasensitive profiles. To determine whether a decoy site with a similar affinity as the activation site could introduce an element of ultrasensitivity, we included a decoy site whose polyproline sequence PPALPPKK

(K_d^{SH3} = 2.1 µM) is near the affinity of the activation site PPALPPKHR (K_d^{SH3} = 2.1 µM)[25] into the synthetic regulatory system (Table 1). The small disparity in affinities between these two sites for the SH3 domain allows the system to exhibit an ultrasensitive response that can be fit to an apparent Hill coefficient of 2.5 (Figure 4C). The decoy site acts as a competitive ligand for the SH3 domain, producing an input threshold where the system is mostly in the decoy-bound state yet allows some SH3 domain binding to the activation site. Modeling of a single-decoy system containing a 2.1 µM decoy (see Supporting Information) generates a sigmoidal input–response curve that closely matches the observed activation profiles (Figure 4C, solid line). We conclude that tuning the affinity of decoy sites so that they are not completely saturated before the activator binds to the activating site can lead to ultrasensitivity.

Ultrasensitive responses have two key characteristics, thresholds and steepness, and we next examined how decoy-based regulatory systems can alter these parameters. For each synthetic regulatory pathway, we defined the threshold as the concentration of activator required to reach 10% output activity and steepness as the slope at the 50% activation point (Figure 5A). As shown in Figure 3, the threshold can be readily manipulated by the addition of decoys, especially with the high affinity (0.1 µM) decoys. We found that steepness, on the other hand, could not be as easily controlled. The inclusion of the lower affinity (2.1 µM) decoy site broadens the input range over which the system transitions between states, requiring more input signal than the no-decoy system to reach maximal activation (Figure 3). After testing several decoy combinations,

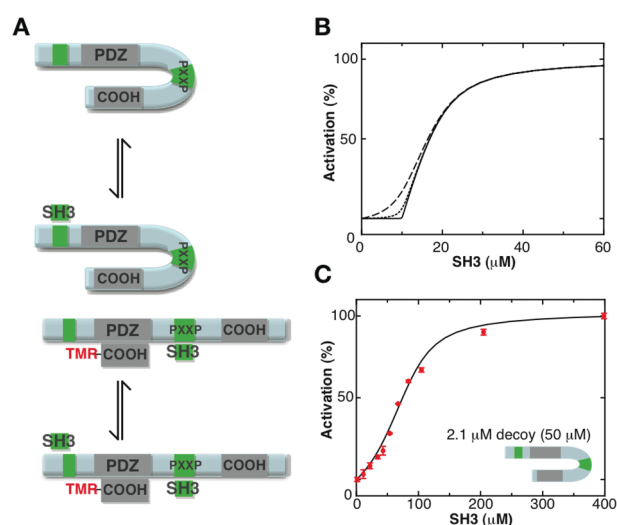**Figure 4.** Decoys can be a source of ultrasensitivity. (A) Graphical representation of end states in the activation sequence (decoy-unbound activated step is omitted for clarity but is included in the analytical modeling in the Supporting Information). The lower-affinity decoy (green) approximates the affinity of the activation site, allowing for mixed binding states. (B) Single-decoy modeling shows that decreasing the affinity of the decoy from nanomolar (solid line) to micromolar affinity (dashed lines) can generate sigmoidal properties. (C) A synthetic regulatory pathway containing a decoy with similar affinity as the activation site (K_d^{SH3} = 2.1 μM, green) for the SH3 domain produces a sigmoidal activation profile and can be fit to an apparent n_H of 2.5 (error bars represent SEM from three independent measurements). The total concentration of the system is 50 μM, which corresponds to a total of 50 μM decoy domains (2.1 μM) and 50 μM repressed polyproline motifs. The solid line represents the predicted behavior of the system based on the analytical model (see Supporting Information) for the system shown in the schematic using the parameters shown in Table 1. It is not the best fit to the data. All affinities used in the modeling correspond to experimentally measured affinities listed in Table 1.

Figure 5. Tailoring response parameters with decoy combinations. (A) Hill coefficients (n_H) are not an accurate measure of the "sensitivity" of a response. The highly thresholded, but less steep curve (red) can be fit to a n_H of 5.1, whereas the steeper but less thresholded curve (black) is fit to a lower n_H of 3.7. Measuring 10% activation (defined as threshold in this work), half-maximal activation (K_{act}), and slope at the steepest part of the curve (dashed line) can clarify ultrasensitive profiles. (B) A synthetic regulatory system containing two 0.1 μM K_d (black) and one 2.1 μM K_d (green) decoy can threshold a sigmoidal activation profile, generating an apparent n_H of 4.5 (note x-axis scale, error bars represent SEM from three independent measurements). The total concentration of the system is 75 μM, which corresponds to a total of 150 μM high affinity decoy domains (K_d^{SH3} = 0.1 μM, black), 75 μM lower-affinity decoy domains (K_d^{SH3} = 2.1 μM, green), and 75 μM repressed polyproline motifs. The solid line represents the predicted behavior of the system based on the analytical model (see Supporting Information) for the system shown in the schematic using the parameters shown in Table 1. It is not the best fit to the data. All affinities used in the modeling correspond to experimentally measured affinities listed in Table 1.

we conclude that the threshold component of ultrasensitive profiles can be readily manipulated in decoy-based regulatory systems, but response steepness is limited to a narrow range.

In addition to steepness and threshold, we also determined each pathway's Hill coefficient, as this term is popularly used to as a measure of ultrasensitivity.[1,2] The Hill coefficient was originally described as a model for cooperativity,[11] and in addition to its use as a measure of ultrasensitivity, it is often used as a measure of activation profile steepness.[12,19] Though steepness does affect the Hill coefficient, we find that increasing the threshold without increasing the steepness can also influence the magnitude of the Hill coefficient (Figure 5B). Therefore, the Hill coefficient may not be the best term to describe how ultrasensitive a system is when other parameters, such as K_{act}, provide a more transparent description of an activation profile. Like the Hill coefficient, K_{act} is also a complex function of the threshold and steepness (Figure 5A) and is defined as the concentration of activator required for 50% activity.[19] Combined, the K_{act}, slope, and threshold offer a complete description of how "ultrasensitive" an activation profile is, as opposed to the Hill coefficient, which can be misleading when thresholds are large.

We have shown that decoys can be used to tune different parameters of a response such as the sensitivity and threshold of a synthetic regulatory pathway *in vitro*. We wanted to expand
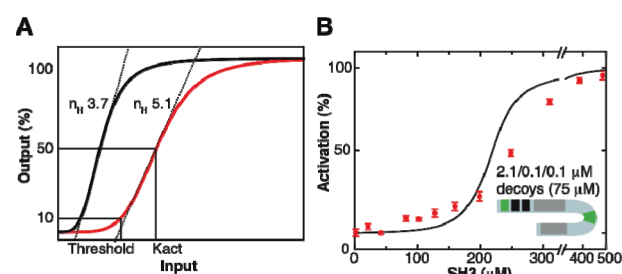
the utility of the synthetic regulatory pathway into a more physiological context, so we introduced the synthetic system into the regulatory pathway that controls mitotic spindle orientation. We chose a cell culture system that uses the cell-adhesion protein Echinoid (Ed) to polarize an otherwise unpolarized S2 cell (Figure 6A).[28] Using this technique, it is possible to polarize any protein of interest in S2 cells, and previous work from our lab has demonstrated that Echinoid fusions of Pins robustly orients the spindle in S2 cells.[28] To explore whether Pins's spindle orientation activity can be altered by decoy-based thresholding, we fused the autoinhibited regulatory system to the cytoplasmic domain of Echinoid to induce crescents of two different synthetic regulatory pathways. We fused the PDZ ligand HREMAVDCP to the C-terminus of soluble Pins and also introduced soluble SH3 as the activator, with the goal of coupling the activation of the regulatory pathway to the spindle orienting activity of Pins (Figure 6B). In this cell culture system, the activation of the regulatory pathway manifests as spindle orientation, which can be plotted as a function of the relative SH3 domain expression level in a given cell.

To determine whether the synthetic regulatory pathway transitions well into the *in vivo* system, we examined the spindle orienting activity of the no-decoy regulatory pathway. Cells expressing relatively low levels of SH3 domain display a broad range of the spindle orientations, suggesting that Pins is not recruited to the induced regulatory pathway crescents (Figure 6C, black circles). However, cells that express higher levels of SH3 domain are restricted to aligned spindle orientation angles, indicating that the regulatory pathway is activated, thereby recruiting Pins to the induced crescents where it functions to orient the spindle. These results demonstrate that the synthetic regulatory pathway can be coupled to spindle orientation.
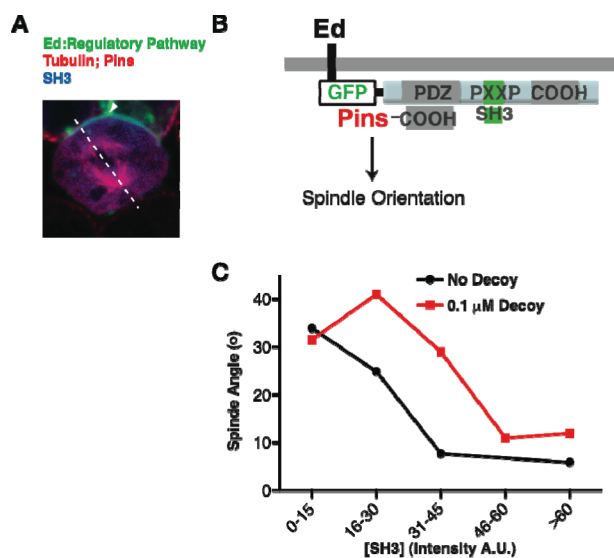
Figure 6. Decoys can threshold spindle orientation activity of Pins. (A) Induced polarity spindle orientation assay. S2 cells adhere through the homophilic, intercellular membrane-associated Echinoid protein (Ed), which redistributes on the cortex to points of cell−cell contact, inducing polarity of the Ed:Regulatory Pathway (shown in green using intrinsic GFP fluorescence). The orientation of the spindle (shown in red with anti-α-tubulin stain) is measured (white dashed line) with respect to the center of the Ed:Regulatory Pathway crescent (white arrowhead). Flag-SH3 expression levels (shown in blue with antiflag antibody, merged with red and green) were determined by measuring the fluorescence intensity of each cell using ImageJ software (see Methods). HA-Pins expression was confirmed by anti-HA antibody stain in red. (B) Regulatory pathways fused to Ed are co-expressed with soluble Pins containing a C-terminal PDZ ligand and soluble SH3 domain in S2 cells. Induced regulatory pathway crescents can be activated by the soluble SH3 molecules, leading to the recruitment of soluble Pins by its C-terminal PDZ ligand fusion. Induced Pins crescents are sufficient to robustly orient the mitotic spindle coupling the activation of the regulatory pathway to spindle orientation. (C) Measurements of the binned intensities (A.U.; intensity corresponds to relative SH3 intracellular concentration) versus spindle orientation angle (deg) of 32 cells expressing the Ed:Regulatory pathway (black, filled circles) and 33 cells expressing the Ed:Regulatory pathway with high-affinity decoy (red, filled squares). Cells were binned at 15 A.U. intensities. Lower spindle angle values represent an aligned phenotype.

To examine the effect of decoys in this system, we tested the spindle orienting activity of a high-affinity 0.1 μM decoy regulatory pathway. Like the no-decoy system, the high-affinity decoy system displays a range of broad spindle orientation angles at low SH3 domain expression levels; however, the random spindle angles persist to higher levels of SH3 domain, indicating that spindle orientation activity is thresholded (Figure 6C, red squares). The high-affinity decoy system finally reaches maximal activation at high SH3 domain expression levels, at about twice the SH3 domain expression level as the no-decoy system. While the thresholding cannot be precisely controlled, as expression levels of all three components are difficult to manipulate, the decoys nevertheless offer some amount of thresholding. Thus, decoy sites can threshold biological activities at the post-translational level through simple binary interactions, and this synthetic regulatory pathway could be adopted for other biological applications.

We have described a strategy to generate ultrasensitivity in a synthetic system utilizing binary protein interactions, where a simple competition mechanism is sufficient to create a sigmoid response curve. We showed that a decoy site, a peripheral domain of the autoinhibited PDZ domain that can bind to the activator, competes with the activation site for the input generating a stoichiometric threshold. Decoy sites with a high affinity for the input generate a threshold that reflects the concentration of the decoy in the system, while still retaining the hyperbolic response of a decoyless system, (i.e., the response is an input-offset hyperbola). When the affinity of the decoy is decreased to approximate the affinity of the activation site for the activator, the system is ultrasensitive and its output follows a sigmoidal path that can be fit to the Hill equation. Finally, because of the modular nature of the synthetic system, we can design systems with desired thresholds and switching efficiencies.

Though the decoy mechanism introduces elements of ultrasensitivity to the system such as thresholds and sigmoidal response curves, it should be noted that the response does not become more steep or switch-like. Despite generating large Hill coefficients, the addition of a competitive decoy reduces the activation slope by a quarter, broadening the range over which the system switches from the inactive to active state, increasing the overall K_{act} of the system. The large apparent Hill coefficients are the result of limitations in describing the two key components of ultrasensitivity, thresholds and steepness. A similar observation was reported in the case of multisite phosphorylation, where multiple phosphorylation sites that act as stoichiometric inhibitors of a kinase introduce a threshold while making the response more graded after the threshold is achieved.[20]

The addition of a high affinity decoy, on the other hand, does not negatively affect the steepness but merely introduces a stoichiometric threshold while retaining the original switch-like transition of the system, which is ultimately determined by the isomerization constant. The response profile could be easily modulated with the addition or removal of these high-affinity decoy domains to achieve a desired input concentration at which the system will abruptly switch from the inactive to active state. This mechanism is also attractive because the modular nature of the decoy system allows the incorporation or removal of domain repeats through genetic recombination events in natural systems. We showed that the synthetic regulatory pathway generated in this study can be adopted in a physiological context and may be useful for other synthetic biologists.

■ METHODS

Protein Construction and Purification. Protein domains were expressed in the *Escherichia coli* BL21(DE3) strain, fused to a cleaveable N-terminal 6×His (pBH4-based vector). The fusion proteins were purified on Ni-NTA resin (Qiagen) and further purified by anion exchange FPLC.

1. SH3 (Activator) and PDZ Domain. The mouse *Crk* (Accession: NP_598417.2) SH3 domain (residues 134−191) was subcloned from vector A5.5a (gift from J. Dueber, UC Berkeley) into the pBH4-based vector *D.melanogaster Par-6* (Accession: NP_573238.1) PDZ domain (residues 156−255) was subcloned by PCR into a pBH4-based vector.

2. Synthetic Regulatory Systems. The PDZ domain of *Par-6* (residues 156−255) was subcloned by PCR and modified by using 5′ and 3′ overhanging primers that introduced desired restriction sites and ligand sequences. The 3′ primer contains a polyproline sequence overlapped with a PDZ-ligand peptide, LPPPALPPKHREMAAD, fusing these overlapping ligands to

the C-terminus of the PDZ domain. The 5′ primer contains sequential *Bam*HI and *Xho*I restriction sites immediately before the first codon of the PDZ domain. Oligonucleotide cassettes encoding various polyproline motifs containing a 5′ *Bam*HI overhang and a 3′ *Xho*I/*Sal*I overhang were ligated to the 5′ end of the PDZ domain. Cassettes were added sequentially in like manner if desired.

3. Peptide Labeling. The peptides CGYPKHREMAVDSP and CGYPKHREMAAD (N-terminally acetylated and C-terminally amidated) were synthesized by EZ-Biolabs. Both peptides' N-terminal cysteines were conjugated to tetramethylrhodamine-maleimide (Invitrogen) as instructed by the manufacturer. Labeled peptides were further purified by RP-HPLC, characterized by MALDI-ToF, and suspended in 0.1% trifluoroacetic acid.

Fluorescence Anisotropy. synthetic regulatory protein at 50, 75, or 100 μM was incubated with 0.5 μM TMR-labeled peptide in binding buffer (20 mM HEPES pH 7.5, 100 mM NaCl, 1 mM DTT). Increasing concentrations of SH3 domain were introduced into the reaction to a final volume of 70 μL. The final reactions were incubated in a 25 °C water bath for 10 min. Anisotropy measurements were conducted using the ISS-PC1 spectrofluorometer equipped with polarizers, with an excitation of TMR at 555 nm and emission recorded at 580 nm over ten iterations (average reading taken). Background anisotropy was measured using SH3 domain alone from 0 to 1 mM; these values served as the baseline for anisotropy background and were subtracted from experimental measurements to obtain "corrected anisotropy" values. Corrected anisotropy values were percentage normalized to the highest and lowest anisotropy values of each synthetic regulatory pathway tested. Fluorescence anisotropy was also used to measure the dissociation constants of the TMR-labeled peptides CGYPKHREMAAD and CGYPKHREMAVDSP for the PDZ domain and repressed PDZ domain. For these measurements, 0−400 μM PDZ domain or repressed PDZ domain was incubated with 0.5 μM of the labeled peptides.

Echinoid Plasmid Construction and Echinoid Cell-Adhesion Assays. Synthetic regulatory systems (see Protein Construction and Purification section 2) were cloned into a pMT/V5-HisA vector (Invitrogen) containing Echinoid and GFP upstream of the multiple cloning site.[28] *Drosophila melanogaster Pins* (Accession: NP_524999.2) residues 1−466, with the C-terminal sequence HREMAVDCP, was cloned into pMT containing an N-terminal HA epitope tag. Mouse *Crk* SH3 residues 134−191 was cloned into pMT containing an N-terminal FLAG epitope tag.

S2 cell maintenance and cell adhesion assays have been detailed elsewhere.[28] Briefly, S2 cells were transfected using Effectene reagent (Qiagen, Germantown, MD) with 1.5 μg total DNA for 24 h. Subsequent protein expression was induced by the addition of 500 μM CuSO$_4$ for 24 h. Cell adhesion clustering was induced by shaking at 175 rpm for 2 h.

Immunostaining, Immunofluorescence Microscopy, and Data Analysis. All synthetic regulatory constructs tested were transfected, fixed, and stained concurrently to minimize variations. Clustered cells were fixed in 4% paraformaldehyde in PBS for 20 min, washed (0.1% saponin in PBS), and incubated with primary antibodies in buffer (0.1% saponin, 1% BSA in PBS) overnight at 4 °C. Coverslips were then washed and incubated with fluorescently linked secondary antibodies for 2 h at room temperature. The coverslips were washed again and

mounted onto microscope slides using Vectashield Hardset medium (Vector Laboratories, Burlingame, CA).

Antibodies were used as follows: rat anti-HA (Roche; 1:1000), rat anti-α-tubulin (Abcam; 1:500), and mouse anti-FLAG (Sigma; 1:1000), Alexa Fluor 555 goat anti-rat IgG (H+L) (Invitrogen; 5 μg/mL), and DyLight 649 AffiniPure Dnk anti-mouse IgG (H+L) (Jackson ImmunoResearch; 7 μg/mL).

All images were collected using a Leica TCS SP2 confocal microscope with a 60X 1.4 NA immersion-oil lens using 488 Ar laser/500−530 nm emission filter, 543 HeNe laser/560−620 nm emission filter, and 633 HeNe laser/650−750 nm emission filter. The refractive index of the immersion oil is 1.518. Laser power, photomultiplier tube gain, and other imaging settings were optimized to fall within the linear range of the camera and to avoid saturation. Optimized settings were held constant throughout imaging sessions.

Fluorescence intensity of a single cell was analyzed using ImageJ software. The inner boundaries of 32−33 cells of each condition were marked using the freehand selection tool and the mean intensity of the marked area was recorded. Background intensity was subtracted from these values. Spindle angles were measured using the angle tool in ImageJ, measuring the spindle angle against the center of the Echinoid crescent. For spindle angle versus intensities plots, cells were binned at 15 A.U. intensity levels.

Analytical Modeling. We modeled binding curves for the no-decoy switch, a one-decoy switch, and a three-decoy switch using constants and concentrations reported in this paper, the curves are not a best fit. All objects, terms, and equations are presented in the Supporting Information. For each switch, we plotted the fraction of the switch bound $f_b p$ to the readout peptide $[P]$ as a function of total activator $[A]_{Tot}$. We used the general binding equation using all states and equilibria to obtain $f_b p$. $[A]_{Tot}$ is presented as the sum of free activator $[A]$ and the summation of all states in which the switch is bound to the activator. In this way, we were able to vary $[A]$ to obtain a $f_b p$ curve as a function of $[A]_{Tot}$.

■ ASSOCIATED CONTENT

⑤ Supporting Information
The objects, terms, and equations used for the analytical modelings of a no-decoy switch, a one-decoy switch, and a three-decoy switch. This material is available free of charge via the Internet at http://pubs.acs.org.

■ AUTHOR INFORMATION

Corresponding Author
*E-mail: prehoda@molbio.uoregon.edu.
Notes
The authors declare no competing financial interest.

■ ACKNOWLEDGMENTS

■ REFERENCES

(1) Koshland, D. E. Jr., Goldbeter, A, and Stock, J. B. (1982) Amplification and adaptation in regulatory and sensory systems. *Science 217* (4556), 220−225.

(2) Ferrell, J. E. Jr. (1996) Tripping the switch fantastic: how a protein kinase cascade can convert graded inputs into switch-like outputs. *Trends Biochem. Sci. 21* (12), 460−466.

(3) Tyson, J. J., Chen, K. C., and Novak, B (2003) Sniffers, buzzers, toggles and blinkers: dynamics of regulatory and signaling pathways in the cell. *Curr. Opin. Cell Biol. 15* (2), 221−231.

(4) Goldbeter, A, and Koshland, D. E. Jr. (1981) An amplified sensitivity arising from covalent modification in biological systems. *Proc. Natl. Acad. Sci. U.S.A. 78* (11), 6840−6844.

(5) Ferrell, J. E. Jr. (1999) Building a cellular switch: more lessons from a good egg. *Bioessays 21* (10), 866−870.

(6) Ferrell, J. E. Jr., and Machleder, E. M. (1998) The biochemical basis of an all-or-none cell fate switch in Xenopus oocytes. *Science 280* (5365), 895−898.

(7) Pomerening, J. R., Sontag, E. D., and Ferrell, J. E. Jr. (2003) Building a cell cycle oscillator: hysteresis and bistability in the activation of Cdc2. *Nat. Cell Biol. 5* (4), 346−351.

(8) Koshland, D. E. Jr., Nemethy, G, and Filmer, D (1966) Comparison of experimental binding data and theoretical models in proteins containing subunits. *Biochemistry 5* (1), 365−385.

(9) Novak, B, and Tyson, J. J. (1993) Numerical analysis of a comprehensive model of M-phase control in Xenopus oocyte extracts and intact embryos. *J. Cell Sci. 106* (Pt 4), 1153−1168.

(10) Buchler, N. E., and Cross, F. R. (2009) Protein sequestration generates a flexible ultrasensitive response in a genetic network. *Mol. Syst. Biol. 5*, 272.

(11) Hill, A (1910) The possible effects of the aggregation of the molecules of haemoglobin on its dissociation curves. *J. Physiol. 40* (Supplemental), iv−vii.

(12) Kim, S. Y., and Ferrell, J. E. Jr. (2007) Substrate competition as a source of ultrasensitivity in the inactivation of Wee1. *Cell 128* (6), 1133−1145.

(13) Pawson, T, and Nash, P (2003) Assembly of cell regulatory systems through protein interaction domains. *Science 300* (5618), 445−452.

(14) Staub, O, and Rotin, D (1997) Regulation of ion transport by protein-protein interaction domains. *Curr. Opin. Nephrol. Hypertens. 6* (5), 447−454.

(15) Mellman, I, and Nelson, W. J. (2008) Coordinated protein sorting, targeting and distribution in polarized cells. *Nat. Rev. Mol. Cell. Biol. 9* (11), 833−845.

(16) Kholodenko, B. N. (2006) Cell-signalling dynamics in time and space. *Nat. Rev. Mol. Cell. Biol. 7* (3), 165−176.

(17) Buchler, N. E., and Louis, M (2008) Molecular titration and ultrasensitivity in regulatory networks. *J. Mol. Biol. 384* (5), 1106−1119.

(18) Smith, N. R., and Prehoda, K. E. (2011) Robust spindle alignment in Drosophila neuroblasts by ultrasensitive activation of pins. *Mol. Cell 43* (4), 540−549.

(19) Dueber, J. E., Mirsky, E. A., and Lim, W. A. (2007) Engineering synthetic signaling proteins with ultrasensitive input/output control. *Nat. Biotechnol. 25* (6), 660−662.

(20) Gunawardena, J (2005) Multisite protein phosphorylation makes a good threshold but can be a poor switch. *Proc. Natl. Acad. Sci. U.S.A. 102* (41), 14617−14622.

(21) Pufall, M. A., and Graves, B. J. (2002) Autoinhibitory domains: modular effectors of cellular regulation. *Annu. Rev. Cell Dev. Biol. 18*, 421−462.

(22) Harris, B. Z., and Lim, W. A. (2001) Mechanism and role of PDZ domains in signaling complex assembly. *J. Cell Sci. 114* (Pt 18), 3219−3231.

(23) Sallee, N. A., Yeh, B. J., and Lim, W. A. (2007) Engineering modular protein interaction switches by sequence overlap. *J. Am. Chem. Soc. 129* (15), 4606−4611.

(24) Penkert, R. R., DiVittorio, H. M., and Prehoda, K. E. (2004) Internal recognition through PDZ domain plasticity in the Par-6-Pals1 complex. *Nat. Struct. Mol. Biol. 11* (11), 1122−1127.

(25) Posern, G, et al. (1998) Development of highly selective SH3 binding peptides for Crk and CRKL which disrupt Crk-complexes with DOCK180, SoS and C3G. *Oncogene 16* (15), 1903−1912.

(26) Wu, X, et al. (1995) Structural basis for the specific interaction of lysine-containing proline-rich peptides with the N-terminal SH3 domain of c-Crk. *Structure 3* (2), 215−226.

(27) Nguyen, J. T., and Lim, W. A. (1997) How Src exercises self-restraint. *Nat. Struct. Biol. 4* (4), 256−260.

(28) Johnston, C. A., Hirono, K, Prehoda, K. E., and Doe, C. Q. (2009) Identification of an Aurora-A/PinsLINKER/Dlg spindle orientation pathway using induced cell polarity in S2 cells. *Cell 138* (6), 1150−1163.